

RESEARCH

Open Access



Moxibustion regulates KDM4D expression and modulates lipid metabolism to inhibit tumor proliferation in CAC mice

Guona Li^{1,2†}, Jindan Ma^{3†}, Luyi Wu¹, Hanxiao Zhang¹, Yaying Lin¹, Hongxiao Xu¹, Muen Gu¹, Kunshan Li², Hongsheng Dong^{2*}, Yan Huang^{1,2*} and Huangang Wu^{1,2*}

Abstract

Background Lysine demethylase 4D (KDM4D) and aberrant lipid metabolism are implicated in the development and progression of colitis-associated cancer (CAC). Moxibustion, a therapeutic approach in traditional Chinese medicine, can inhibit intestinal inflammation and improve the intestinal mucosa.

Methods Mice were intraperitoneally injected with AOM, and three cycles of 3–2–2% DSS-free drinking water were administered to establish a CAC mouse model. Moxibustion and KDM4D inhibitor 5-c-8HQ intervention were performed for 30 days after modeling was completed. IHC staining was used to observe the expression of the nuclear-associated antigen Ki67 (Ki67), proliferating cell nuclear antigen (PCNA), and IL-33 in the colon. The expression of colon KDM4D and β -Catenin was observed by immunofluorescence staining and RT-qPCR. LC-MS pseudotargeted metabolomic sequencing was used to semiquantitatively detect the expression levels of lipids.

Results Moxibustion inhibited the proliferation of colon tumors in CAC mice, improved histopathology, and reduced the expression of PCNA and Ki67 in the colon. Using *kdm4d* knockout technology, it was initially confirmed that *kdm4d* is a key gene affecting CAC tumor proliferation. The inhibition of colon tumor proliferation in CAC mice by moxibustion is associated with the suppression of abnormal activation of the colon KDM4D/ β -Catenin signaling pathway. LC-MS-targeted metabolomics revealed abnormal lipid metabolism in the colons of CAC mice. Moxibustion may affect the cholinergic metabolism pathway in the colon of CAC mice and regulate lipids such as sphingomyelin SM (d18:1/26:0) and triacylglycerol TAG58:7 (18:0). After *kdm4d* knockout, lipid disorders in the colons of CAC mice were partially restored. The *kdm4d* gene may be involved in the mechanism underlying the effect of moxibustion on lipid metabolism in the CAC colon.

[†]Guona Li and Jindan Ma contributed equally to this work.

*Correspondence:
Hongsheng Dong
dhsdoctor2005@126.com
Yan Huang
huangyan@shutcm.edu.cn
Huangang Wu
wuhuangang@shutcm.edu.cn

Full list of author information is available at the end of the article



© The Author(s) 2025. **Open Access** This article is licensed under a Creative Commons Attribution-NonCommercial-NoDerivatives 4.0 International License, which permits any non-commercial use, sharing, distribution and reproduction in any medium or format, as long as you give appropriate credit to the original author(s) and the source, provide a link to the Creative Commons licence, and indicate if you modified the licensed material. You do not have permission under this licence to share adapted material derived from this article or parts of it. The images or other third party material in this article are included in the article's Creative Commons licence, unless indicated otherwise in a credit line to the material. If material is not included in the article's Creative Commons licence and your intended use is not permitted by statutory regulation or exceeds the permitted use, you will need to obtain permission directly from the copyright holder. To view a copy of this licence, visit <http://creativecommons.org/licenses/by-nc-nd/4.0/>.

Conclusions Moxibustion inhibited the proliferation of colon tumors in CAC mice, inhibited the activation of the tumor-promoting signaling pathway KDM4D/ β -Catenin, and improved lipid metabolism disorders in the colon, thus providing a promising strategy for the clinical adjuvant treatment of colorectal cancer.

Keywords Colitis-associated cancer, Moxibustion, KDM4D, β -Catenin, Lipid metabolism

Introduction

Colorectal cancer (CRC) is a common malignant tumor of the digestive system [1]. Epidemiological data have revealed that CRC is the second leading cause of cancer-related death, accounting for 8.6% of all cancer-related deaths [2]. Moreover, the incidence of CRC in young patients has also increased. Since 2010, the incidence of CRC among people under 65 years of age has increased by approximately 1–2% annually [3]. Inflammation is a characteristic of tumors. Chronic inflammation can cause DNA damage and promote tumor progression [4]. Conversely, the pathogenesis of tumors involves continuous inflammation [4]. Inflammatory bowel disease (IBD) is characterized by recurrent intestinal inflammation. Chronic inflammation and epithelial cell proliferation lead to the development of low-grade and high-grade dysplasia, which may further transform into colitis-associated cancer (CAC) [5]. Ulcerative colitis (UC) and Crohn's disease (CD) are the two most common types of IBD. The risk of colorectal cancer in patients with UC has been reported to increase approximately 2–3-fold [6]. Therefore, it is crucial to elucidate the potential mechanism of colonic inflammation and cancer transformation, delay the proliferation of CAC tumor cells, and reduce the occurrence of colon tumors.

Lysine demethylase 4D (KDM4D), also known as JMJD2D, is a member of the KDM4 subfamily of histone lysine demethylases (KDMs) and participates in various posttranslational modification processes in cells [7]. KDM4D has been proven to be a recognized epigenetic promoter in the progression of various malignant tumors, especially CRC and hepatocellular carcinoma [8, 9]. KDM4D can also interact with β -Catenin as a coactivator and promote H3K9me3 modification of the downstream oncogenes MYC, MMP9, MMP2, and cyclin D1, inducing the proliferation of tumor cells [10]. However, when the expression of KDM4D is inhibited by the KDM4D inhibitor 5-chloro-8-hydroxyquinoline (5-c-8HQ), the expression of β -Catenin, MYC, and cyclin D1 in colorectal cancer tumor cells and tissues is reduced, and the proliferation of tumor cells is also inhibited [10, 11].

Lipids are important components of the cell and organelle membranes. Lipid metabolism not only supports energy production but also plays an important role in biosynthetic pathways and redox homeostasis. Fatty acids are involved in multiple pathways related to tumor cell proliferation, differentiation, and immune drug resistance [12]. Lipogenesis, increased lipid content, and

lipid-dependent catabolism can also lead to chemotherapeutic desensitization and drug-resistant phenotypes in tumor cells [13]. The lipid metabolism pathways of tumor cells are regulated by multiple signaling pathways, such as the Wnt, Notch, Hippo, and Hedgehog pathways. Therefore, exploring the interaction between the KDM4D/ β -Catenin signaling pathway and lipid metabolism is pivotal for further understanding the pathogenesis of CAC.

As a traditional Chinese medicine treatment method, moxibustion is widely used in clinical practice and achieves therapeutic effects by burning moxa at specific acupoints. Several studies have shown that the use of moxibustion as an adjuvant therapy can treat a wide range of cancer-related complications, including gastrointestinal symptoms, bone marrow suppression, fatigue, pain and lymphedema [14, 15]. Our previous studies demonstrated that moxibustion can effectively reduce DSS-induced colonic injury and inflammation [16]. Moxibustion can also reduce the colonic tumor load in rats, regulate the abnormal expression of KDM4D, and inhibit the abnormal activation of Wnt/ β -Catenin [17]. To date, no study has explored the effect of moxibustion on CAC tumor proliferation from the perspective of regulating KDM4D/ β -Catenin and lipid metabolism. Therefore, in this study, we selected wild-type C57BL/6J and *kdm4d* knockout mice and used azoxymethane (AOM) combined with dextran sulfate sodium (DSS) to construct a CAC model to explore the effects of moxibustion on colon tumor proliferation, the KDM4D/ β -Catenin signaling pathway, and lipid metabolism in CAC mice.

Methods

Animals

SPF grade wild-type (WT) C57BL/6J mice (male, 4–5 weeks) were purchased from Shanghai Model Organisms Center, Inc. SPF-grade *kdm4d* gene knockout (KO) mice (4–5 weeks) with a C57BL/6J genetic background were purchased from Jackson Laboratory (Supplementary Fig. S1). The mice were housed in the Laboratory Animal Center of Shanghai University of Traditional Chinese Medicine (SHUTCM). The breeding environment included an alternating 12-hour day–night cycle, a room temperature of 20 ± 2 °C, a humidity of 50–70%, and free access to food and water. All operations were approved by the SHUTCM (No. PZSHUTCM2305180004 and PZSHUTCM220725005), which is completed with relevant regulations on animal ethics.

CAC model establishment

After one week of adaptive feeding, the mice were randomly divided into a normal control group (NC), a CAC group, a moxibustion group (MOX), and a KDM4D inhibitor 5-c-8HQ group. AOM combined with DSS was used to establish the CAC model [18]. On the first day, the mice were intraperitoneally injected with AOM (10 mg/kg, A5486, Sigma). One week later, three cycles of chronic inflammatory stimulation with 3-2-2% DSS

(9011-18-1, MP) were administered. In the first cycle (from day 8 to day 28), the mice had free access to 3% DSS for four days, followed by normal drinking water for 17 days. In the second cycle (from days 29 to 49), the mice had free access to 2% DSS for 4 days, followed by normal drinking water for 17 days. The drinking water scheme for the second cycle was repeated in the third cycle (Fig. 1A). After model establishment, two normal control mice and two model mice were randomly

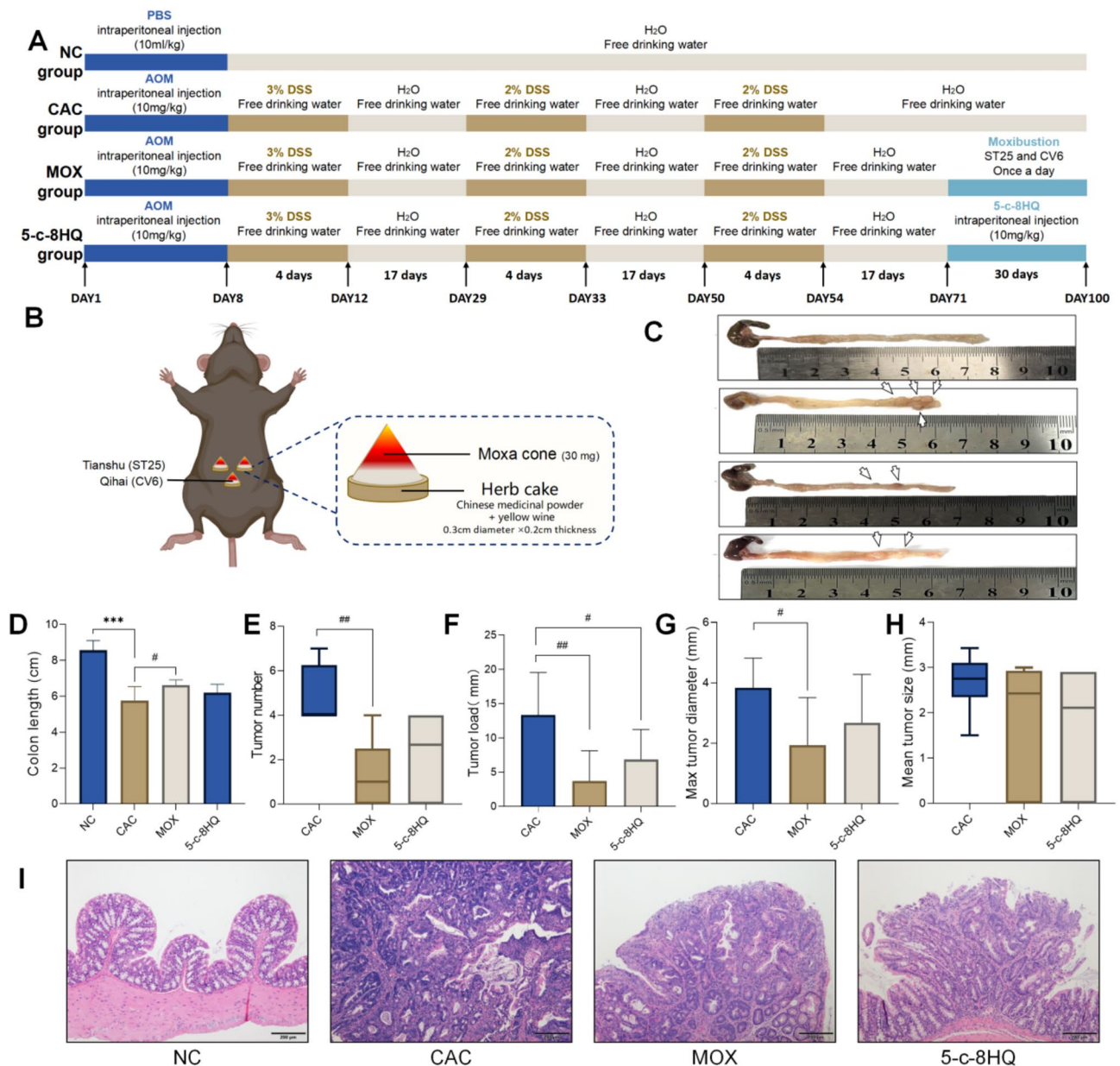


Fig. 1 Effects of moxibustion on colon tumorigenesis in CAC mice. **A** schematic protocol for the experiments: AOM (10 mg/kg) via intraperitoneal injection combined with 3 cycles of DSS-free drinking water was used to establish the CAC mouse model, and the mice were subsequently subjected to moxibustion or 5-c-8HQ interventions. **B** Schematic diagram of the moxibustion operation. **C** Macroscopic observation of the colons of the mice in each group; the formation of colonic tumors is indicated by white arrows. **D-H** Comparison of colon length, tumor number, tumor load, maximum tumor diameter and mean tumor diameter. **I** H&E staining of the colons of the mice in each group (scale bars, 200 μm). *n*=6, compared with the NC group, ****P*<0.001; compared with the CAC group, #*P*<0.05

selected for model identification (Supplementary Figs. S2 and S3). The success of establishing the CAC model was evaluated by gross observation and HE staining.

Moxibustion and 5-c-8HQ intervention

Moxibustion and 5-c-8HQ intervention were performed the day after modeling was completed. Herb cake was created from Chinese medicinal powder (Shanghai Huaji Pharmaceutical Co., Ltd., China) and yellow wine, with a thickness of approximately 0.2 cm and a diameter of approximately 0.3 cm. These herbs were placed on the *Qihai* (CV6) and bilateral *Tianshu* (ST25) acupoints, with a moxa cone (approximately 30 mg, Nanyang Hanyi Moxa, China) positioned on top of each cake. Two moxa cones were applied to each acupoint once daily for 30 d (Fig. 1B). 5-c-8HQ is an inhibitor of KDM4D [19]. The mice in the 5-c-8HQ group received intraperitoneal injections of 5-c-8HQ (10 mg/kg, HY-12304, MCE) once daily for 30 d [10]. Mice in the normal and CAC groups underwent the same grasping and fixation procedures as those in the moxibustion group did. No deaths occurred in the mice during the experimental period.

Observation of colon tumorigenesis

After the intervention, the mice in each group were fasted for 12 h without water restriction. After intraperitoneal anesthesia with 1% pentobarbital sodium (0.4–0.5 ml/100 g), the mice were sacrificed by cervical dislocation. The abdominal cavity was opened, and the colon tissue was removed from the pubic symphysis to the cecum. The colon tissue was stripped cleanly on ice, cut longitudinally, rinsed, and photographed. Colon length was recorded, and tumorigenesis of the mucosal tumor was observed. The tumor number was the number of tumors observed grossly in the colon of a single mouse. The average tumor diameter was the mean value of all tumor diameters observed in the colons of the mice. The tumor burden was the sum of the diameters of all the tumors in the colons of the mice.

Hematoxylin–eosin (HE) staining

Colonic tissues were selected according to colon tumorigenesis; one part was used for immunofluorescence and immunohistochemistry detection, and the other part was used for mRNA and lipid metabolomic detection. Mouse colon tissue was dehydrated, fixed in 4% paraformaldehyde, paraffin-embedded after fixation, and sectioned at a thickness of 4 μ m. HE staining was used to observe the histopathological changes in the colon tissue and the epithelium of the colon intestinal mucosa, intestinal glands, and infiltration of inflammatory cells. The presence or absence of heterogeneous hyperplasia and the generation of adenocarcinoma were observed.

Immunohistochemistry (IHC) staining

IHC staining was used to observe the expression of the Ki67, PCNA, and IL-33 in the colons of the mice in each group. Paraffin-embedded tissues were cut into 4- μ m-thick sections and deparaffinized with xylene and ethanol. Trisodium citrate and citric acid were used to prepare the antigen repair solutions. The slides were placed in 3% H₂O₂ solution to inactivate endogenous antibodies. A 3% bovine serum albumin (BSA) solution was added inside the organizing circle and incubated at room temperature for 30 min. The blocking solution was shaken, and PBS-diluted primary antibodies (Anti-Ki67, GB121141, Servicebio, China, 1:500; Anti-PCNA, 13110, Cell Signaling, USA, 1:4000; Anti-IL-33, PA596929, Thermo Fisher, USA, 1:250) were added, followed by incubation at 4 °C overnight. After incubation with the secondary antibody, DAB was used for color development, and the nuclei were stained with hematoxylin. The sections were then dehydrated with ethanol and sealed with neutral gum. IHC staining results were observed using a light microscope (BX53, OLYMPUS). Three positively stained areas were randomly selected, the average optical density (AOD) values were calculated using ImageJ software, and the mean values were used to semi-quantify protein expression.

Immunofluorescence staining

The expression of colon KDM4D and β -Catenin was observed by immunofluorescence staining. The sections were then deparaffinized and rehydrated. The antigen retrieval solution was prepared with citric acid, and endogenous antibodies were inactivated with 3% H₂O₂ solution and blocked with 3% BSA solution. A mixture of primary antibodies diluted in PBS (KDM4D, sc-393750, Santa Cruz, USA, 1:200; β -Catenin, GB15015, Servicebio, China, 1:1000) was added and incubated overnight at 4 °C in a wet box. The sections were subsequently incubated with an Alexa Fluor 488-labeled goat anti-mouse IgG secondary antibody (GB25301, Servicebio), incubated at room temperature for 50 min, and then washed with PBS. After drying, CY3-labeled goat anti-rabbit IgG secondary antibody (GB21303, Servicebio) was added, and the mixture was incubated at room temperature in the dark. DAPI staining solution was used to counterstain the nuclei. Images were captured using a fluorescence microscope and microscope slide scanner (NIKON ECLIPSE C1, Nikon; Panoramic MIDI, 3DHISTECH).

RT–qPCR

The expression levels of KDM4D and β -Catenin mRNAs in colon tumors were detected via RT–qPCR. Total RNA was extracted via a TRIzol kit (15596018, Invitrogen, USA), and the RNA concentration was determined using RNA ultraviolet photometry. In this reaction system, the

RNA was reverse-transcribed into cDNA. The reaction mixture was prepared on ice (TB Green Premix Ex Taq 10 μ l + PCR forward primer 10 μ mol 0.4 μ l + PCR reverse primer 10 μ mol 0.4 μ l + cDNA 2 μ l + ddH₂O 7.2 μ l). PCR was used for amplification. The program was set as follows: 95 °C for 30 s, 1 cycle; 95 °C for 5 s, 60 °C for 30 s, 40 cycles; 95 °C for 5 s, 60 °C for 1 min, 95 °C for 1 cycle; and 50 °C for 30 s, 1 cycle. The amplification and melting curves were confirmed, the CT value of each sample was obtained, and the expression of mRNA was calculated using the $2^{-\Delta\Delta CT}$ method. The primer sequences for KDM4D and β -Catenin are listed in Table S1.

Detection and analysis of LC-MS lipid metabolism profiles

LC-MS pseudotargeted metabolomic sequencing was used to semiquantitatively detect the expression levels of five categories (sterol lipids, fatty acids, glycerophospholipids, glycerides, and sphingolipids) and 30 subcategories of lipid substances in the colons of the mice in each group. The chromatographic conditions were as follows: column temperature, 55 °C; mobile phase A, acetonitrile: water (60:40, v/v); mobile phase B, acetonitrile: isopropanol (10:90, v/v); flow rate, 0.35 mL/min; and injection volume, 5 μ L. The Qtrap6500 plus mass spectrometry detection system (AB Sciex, USA) was used to perform high-throughput analysis of more than 1000 lipid substances in schedule-MRM mode. The mass spectrometry conditions were as follows: curtain gas, 40 psi; ion spray voltage, -4500/5500 V; source temperature, 400 °C; nebulizing gas, 50 psi; and auxiliary heating gas, 55 psi. Quality control of the lipid sequencing data was performed (Supplementary Fig. S4). The lipid metabolism sequencing results were analyzed using bioinformatics methods such as principal component analysis (PCA), cluster analysis (volcano plot and heatmap), differentially abundant metabolite screening, and Kyoto Encyclopedia of Genes and Genomes (KEGG) pathway analysis.

Statistical analysis

Statistical analysis and visualization were performed using SPSS 26.0 and GraphPad 9.0. One-way ANOVA was used to analyze normally distributed data statistically. According to the homogeneity of variance results, the LSD method or Dunnett's T3 method was used for intergroup tests. Nonparametric tests were used to analyze nonnormally distributed data. $P < 0.05$ was considered statistically significant.

Results

Moxibustion suppresses AOM plus DSS-induced tumorigenesis in CAC mice

Intraperitoneal injection of AOM (10 mg/kg) combined with free access to DSS for three cycles led to weight loss, diarrhea, bloody stools, and prolapse in the mice. Gross

observation and HE staining of the colon revealed tumor formation in the colonic mucosa and shortening of the colon (Supplementary Fig. S2). These results are consistent with those of previous studies, indicating the successful establishment of a mouse CAC model [20, 21]. We performed moxibustion on the *Qihai* (CV6) and bilateral *Tianshu* (ST25) acupoints in the MOX group and an intraperitoneal injection of 5-c-8HQ in the KDM4D inhibitor 5-c-8HQ group (Fig. 1A-B). After the intervention was completed, the colon tissues of the mice in each group were removed and longitudinally incised. The colonic mucosa of the mice in the NC group was intact, and no mucosal congestion, edema, ulcers, or tumor formation was observed. Tumor formation was visible in the colons of the mice in the other groups (Fig. 1C). First, we observed the effects of moxibustion and 5-c-8HQ on tumorigenesis in mice with CAC. As shown in Fig. 1D-H, compared with those in the CAC group, the number of colon tumors, tumor load, and maximum tumor diameter in the MOX group were significantly lower ($P < 0.05$), and the colon length was significantly increased ($P < 0.05$). Compared with that in the CAC group, the tumor load in the 5-c-8HQ group was significantly lower ($P < 0.01$). HE staining revealed that after moxibustion and 5-c-8HQ treatment, the typical pathological changes in the colon of CAC mice were alleviated, with improved gland arrangement and reduced infiltration of inflammatory cells (Fig. 1I). These results suggest that moxibustion and the KMD4D inhibitor can reduce the colonic tumor burden in CAC mice and that moxibustion has advantages in reducing the number of colonic tumors and reducing the tumor size in CAC mice.

Moxibustion inhibits the expression of tumor proliferation proteins in CAC mice

We used immunohistochemical staining to observe the effects of moxibustion on the expression of PCNA, Ki67 and IL-33 in the colon of CAC mice. Compared with those in the NC group, the AOD values of Ki67 and PCNA in the colons of the mice in the CAC group were significantly increased ($P < 0.05$). Compared with those in the CAC group, the AOD values of Ki67 and PCNA in the colons of the mice in the MOX and 5-c-8HQ groups were significantly lower ($P < 0.05$) (Fig. 2A-B, D-E). Under the stimulation of repeated drinking of DSS, the colon exhibited chronic inflammation. Compared with that in the NC group, the AOD value of IL-33 in the colon of the mice in the CAC group was significantly increased ($P < 0.05$). Compared with that in the CAC group, the AOD value of IL-33 in the colon of mice in the MOX and 5-c-8HQ groups was significantly lower ($P < 0.05$) (Fig. 2C and F). These results suggest that moxibustion can inhibit the proliferation of CAC tumor cells and reduce intestinal inflammation.

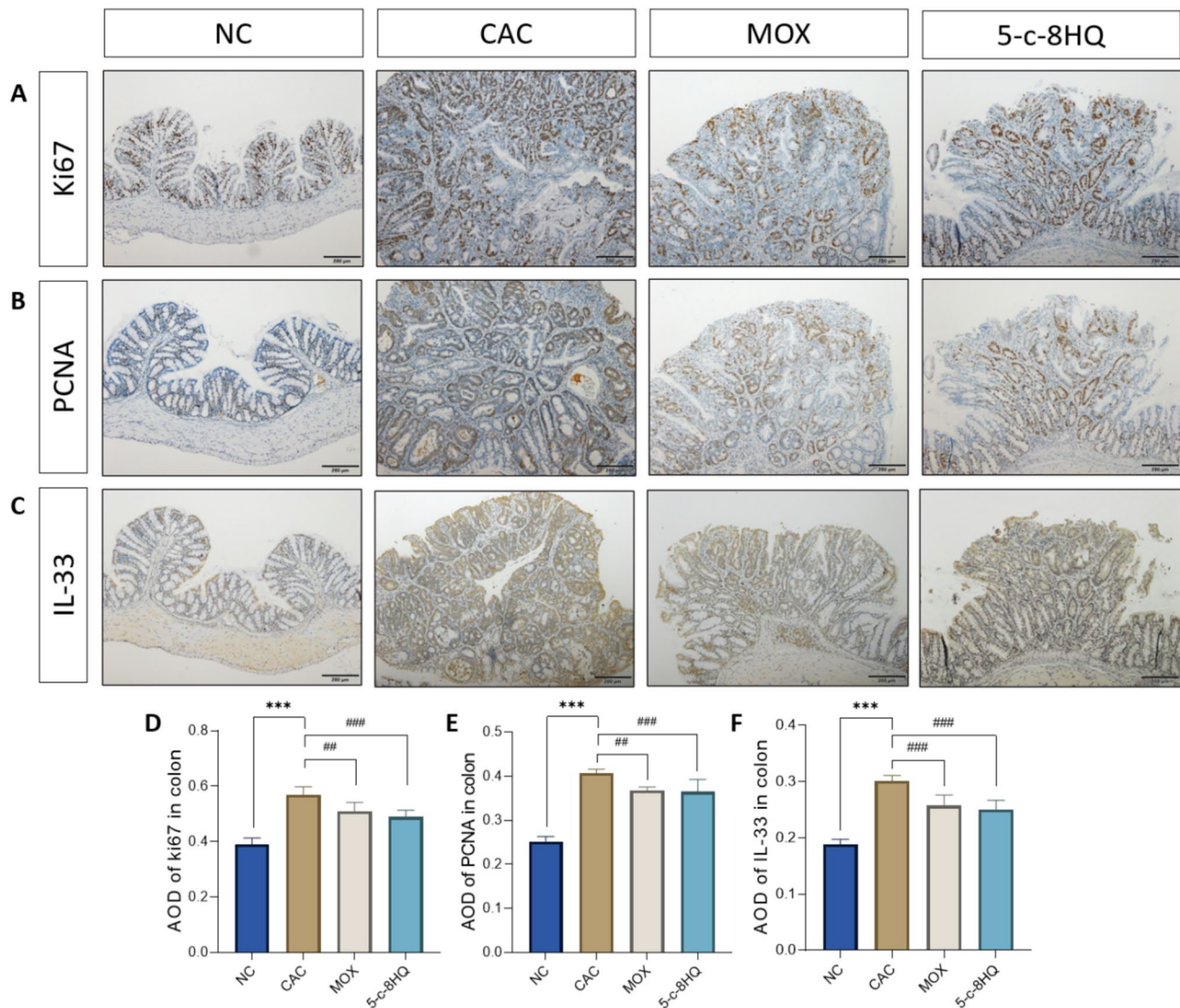


Fig. 2 Effects of moxibustion on the expression of proliferation-related proteins and IL-33 in CAC tumors. **A-C** Ki67, PCNA and IL-33 expression in colon tumors (scale bars, 200 μ m). **D-F** AOD values of Ki67, PCNA and IL-33 in colon tumors. $n=6$, compared with the NC group, *** $P<0.001$; compared with the CAC group, ** $P<0.01$, ### $P<0.001$

Moxibustion reduces the coexpression of KDM4D and β -Catenin in the colons of CAC mice

To explore whether the effect of moxibustion to inhibit the proliferation of colon tumors in CAC mice is related to the regulation of KDM4D and β -Catenin expression, we detected the mRNA expression and protein coexpression of KDM4D and β -Catenin in the colons of the mice in each group. The immunofluorescence results revealed that the fluorescent signals of KDM4D and β -Catenin appeared mainly in the mucosal layer. Compared with that in the NC group, the fluorescence intensity of KDM4D and β -Catenin in the colon tissue of mice in the CAC group was greater in colon tumors with yellow fluorescent coexpression. Compared with those in the CAC group, the fluorescence intensities of KDM4D and

β -Catenin in the colons of the mice in the MOX and 5-c-8HQ groups were lower (Fig. 3A). The RT-qPCR results revealed that, compared with those in the NC group, the relative expression levels of KDM4D and β -Catenin mRNAs in the colon tumors of the mice in the CAC group were significantly greater ($P<0.05$). Compared with those in the CAC group, the relative expression levels of KDM4D and β -Catenin mRNAs in the colon tumors of the mice in the MOX and 5-c-8HQ groups were significantly lower ($P<0.05$) (Fig. 3B-C). These results suggest that moxibustion can reduce the colonic tumor burden and inhibit the expression of KDM4D and β -Catenin in the colon tumors of CAC mice (Fig. 3D).

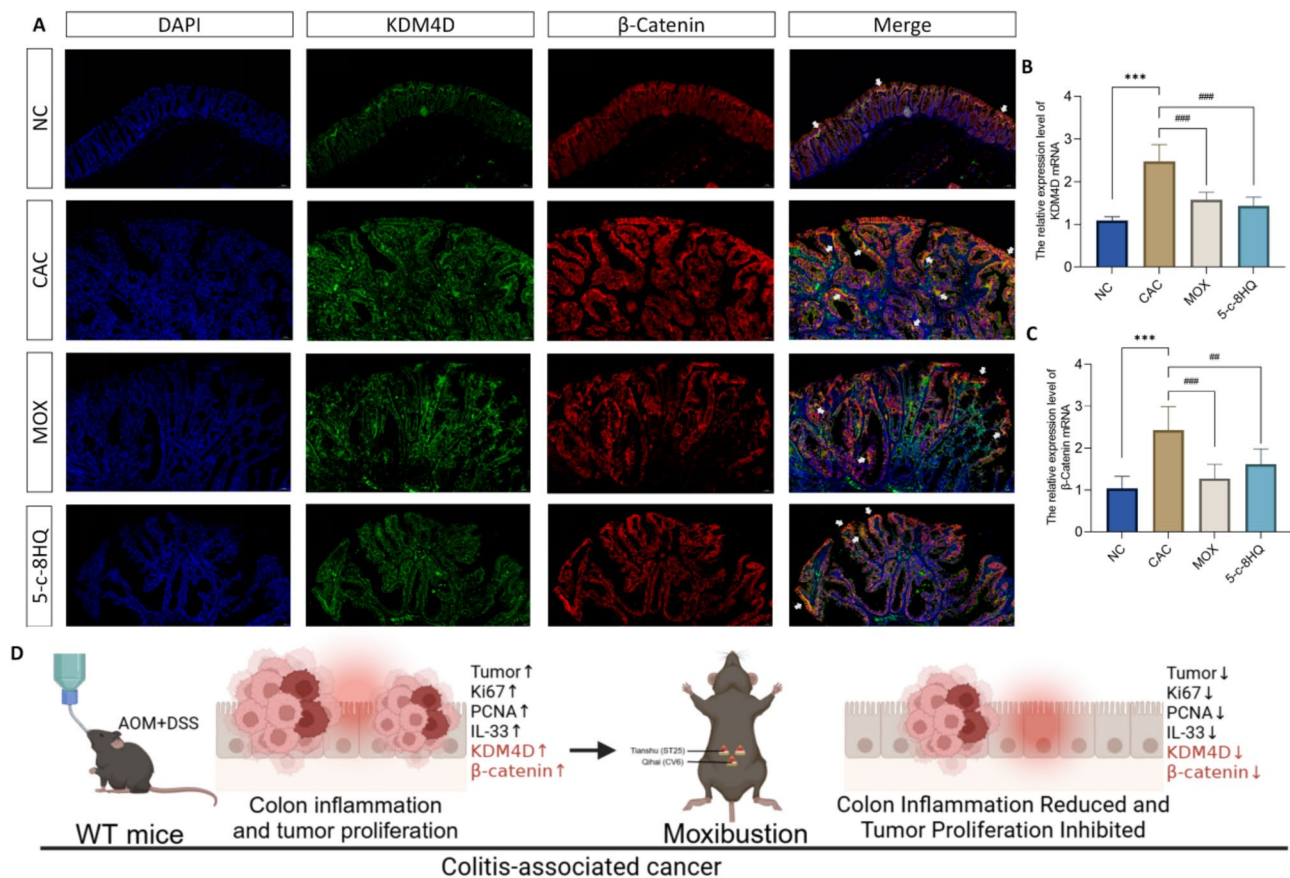


Fig. 3 Effects of moxibustion on the protein and mRNA expression of KDM4D and β-Catenin in CAC tumors. **A** KDM4D and β-Catenin expression in colon tumors (scale bars, 50 μm); white arrows indicate the coexpression of KDM4D and β-Catenin. **B-C** Relative expression levels of KDM4D and β-Catenin mRNAs in colon tumors. **D** Graphical illustration of the overall effect of moxibustion on CAC mice. $n=6$, compared with the NC group, $***P<0.001$; compared with the CAC group, $##P<0.01$, $###P<0.001$

The effect of moxibustion on colonic lipid metabolism in CAC mice

To explore whether moxibustion affects colonic lipid metabolism in CAC mice, we performed LC-MS lipid metabolomic analysis of mouse colon tissues. PCA and heatmaps revealed differences in colonic lipid metabolism among the WT-NC, WT-CAC, and WT-MOX groups (Fig. 4A-B). Differentially expressed lipid metabolites between groups were screened using a fold change (FC) of >1.2 or <0.83 and $P<0.05$. The results of the volcano plot revealed that, compared with those in the WT-NC group, 69 lipid metabolites were significantly upregulated in the colons of the WT-CAC group, while 154 lipid metabolites were significantly downregulated. Compared with those in the WT-CAC group, 22 significantly upregulated lipid metabolites and 17 significantly downregulated lipid metabolites were detected in the colons of the WT-MOX group (Fig. 4C-D).

The KEGG database was used for pathway enrichment analysis of differentially expressed lipid metabolites between the groups. As shown in Fig. 4E and F, the main enriched KEGG pathways of differentially expressed lipid

metabolites between the WT-NC and WT-CAC groups included basal cell carcinoma, the neurotrophin signaling pathway, the adipocytokine signaling pathway, fat digestion and absorption, choline metabolism in cancer, lipid and atherosclerosis, the sphingolipid signaling pathway, and glycerophospholipid metabolism. The KEGG pathways associated with the differentially expressed lipid metabolites between the WT-CAC and WT-MOX groups were enriched mainly for autophagy, choline metabolism in cancer, glycerophospholipid metabolism, and linoleic acid metabolism.

Next, we screened the lipid targets of moxibustion-inhibiting CACs via Venn diagrams. Compared with those in the WT-NC group, 20 lipids were downregulated in the WT-CAC group and upregulated in the colon of the WT-MOX group (Fig. 4G). Compared with those in the WT-NC group, five lipids were upregulated in the WT-CAC group but downregulated in the WT-MOX group (Fig. 4H). Among the 25 lipids at the intersection, 10 were significantly different between the groups (Fig. 4I).

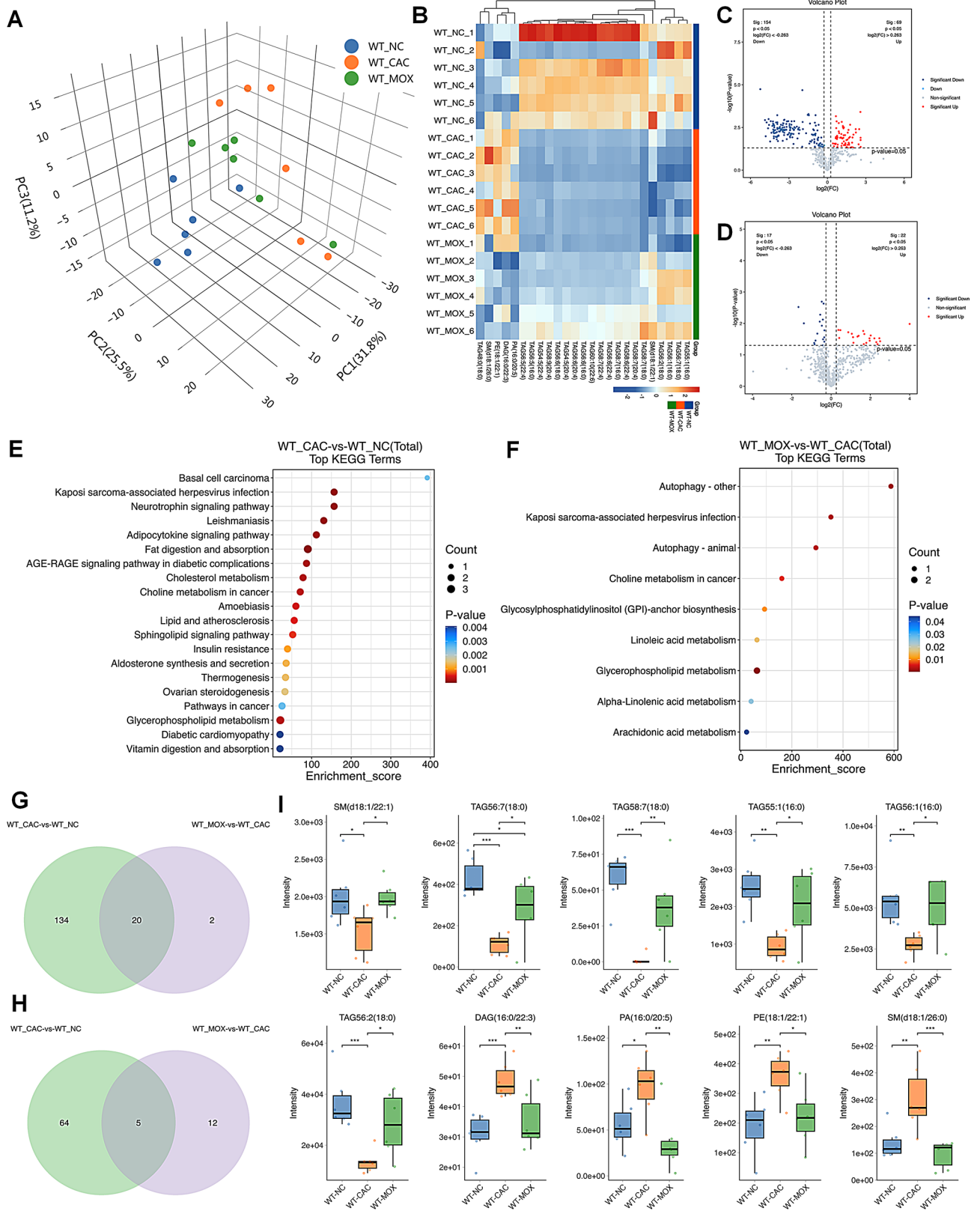


Fig. 4 (See legend on next page.)

(See figure on previous page.)

Fig. 4 Effects of moxibustion on lipid metabolism in CAC tumors. **A** 3D-PCA diagram. **B** Heatmap of lipid metabolism in the three groups. **C** Volcano plot of differential lipids between the WT-NC group and the WT-CAC group. The red dots represent lipids upregulated in the WT-CAC compared with the WT-NC, and the blue dots represent lipids downregulated in the WT-CAC compared with the WT-NC. **D** Volcano plot of differential lipids between the WT-CAC group and the WT-MOX group. The red dots represent lipids upregulated in WT-MOX compared with WT-CAC, and the blue dots represent lipids downregulated in WT-MOX compared with WT-CAC. **E** KEGG enrichment pathway analysis of differential lipids between the WT-NC group and the WT-CAC group. **F** KEGG enrichment pathway analysis of differential lipids between the WT-CAC group and the WT-MOX group. **G** Venn diagram of lipids significantly downregulated in the WT-CAC group compared with the WT-NC group and significantly upregulated in the WT-MOX group compared with the WT-CAC group. **H** Venn diagram of lipids significantly upregulated in the WT-CAC group compared with the WT-NC group and significantly downregulated in the WT-MOX group compared with the WT-CAC group. **I** Box plot of differential lipids in the three groups of mice. $n=6$, $^*P<0.05$, $^{**}P<0.01$, $^{***}P<0.001$

Compared with those in the WT-NC group, the levels of sphingomyelin SM(d18:1/22:1), TAG56:7(18:0), TAG58:7(18:0), TAG55:1(16:0), TAG56:1(16:0), and TAG56:2(18:0) in the colons of the WT-CAC group were significantly lower ($P<0.05$). Compared with those in the WT-CAC group, the contents of the above mentioned lipids were significantly greater in the WT-MOX group ($P<0.05$). Compared with those in the WT-NC group, the levels of diacylglycerol DAG(16:0/22:3), phosphatidic acid PA(16:0/20:5), phosphatidylethanolamine PE(18:1/22:1), and SM(d18:1/26:0) in the colons of the WT-CAC group were significantly increased ($P<0.05$). However, compared with those in the WT-CAC group, the contents of these lipids were significantly lower in the WT-MOX group ($P<0.05$). These results suggest that lipids such as SM(d18:1/22:1) may be lipid metabolite targets for moxibustion to inhibit colon tumors in CAC mice.

Effect of *kdm4d* knockout on tumor proliferation in CAC mice

To explore the role of KDM4D in the proliferation of colon tumors in CAC mice, we constructed *kdm4d* knockout (*kdm4d*^{-/-}) mice (Fig. 5A). After *kdm4d*, AOM combined with DSS induced colon tumor formation in the mice (Fig. 5B). Compared with those in the WT-CAC group, the number of tumors and tumor load in the KO-CAC group were significantly lower ($P<0.05$), while there were no statistically significant differences in colon length, maximum number of tumors, or average number of tumors (Fig. 5D-H). HE staining revealed that the degree of atrophy and fusion of colonic glands in the KO-CAC group was greater than that in the WT-CAC group (Fig. 5C). Compared with those in the WT-CAC group, the AOD values of Ki67, PCNA, and IL-33 in the colon tumors of the mice in the KO-CAC group were significantly lower ($P<0.05$) (Fig. 5I-L). These findings suggest that *kdm4d* knockout can inhibit tumor proliferation and inflammation.

β -Catenin expression in the colon is shown in Fig. 5M-N. Immunofluorescence staining revealed that, compared with that in the WT-CAC group, the fluorescence intensity of β -Catenin in the colons of the KO-CAC group was lower. Compared with that in the WT-CAC group, the

relative expression level of β -Catenin mRNA in the colons of the mice in the KO-CAC group was significantly lower ($P<0.05$). These results suggest that *kdm4d*^{-/-} mice have significantly reduced β -Catenin expression in the colon. β -Catenin may be a key downstream signal of KDM4D.

The effect of moxibustion on tumorigenesis in *kdm4d*^{-/-} knockout mice

To explore whether KDM4D is involved in the process by which moxibustion inhibits CAC tumor proliferation, we examined the regulatory effects of moxibustion on tumorigenesis in *kdm4d*^{-/-} mice (Fig. 6A). As shown in Fig. 6B, in the KO-CAC and KO-MOX groups, AOM combined with DSS also led to the formation of colon tumors in the mice. Compared with those in the KO-NC group, the colon lengths of the mice in the KO-CAC group were significantly shorter ($P<0.01$) (Fig. 6C). However, there were no statistically significant differences between the KO-MOX group and the KO-CAC group in terms of the number of tumors, tumor load, mean tumor size, maximum tumor diameter or colon length (Fig. 6C-G). HE staining revealed mild inflammatory cell infiltration and dysplasia in the colons of the mice in the KO-CAC and KO-MOX group (Fig. 6H). These results suggest that moxibustion did not significantly inhibit tumor proliferation in *kdm4d*^{-/-} mice. KDM4D may act as a signaling molecule for moxibustion to inhibit the proliferation of CAC tumors in mice.

In *kdm4d*^{-/-} mice, moxibustion does not reduce the expression of β -Catenin in CAC colonic tumors

The immunohistochemical results are shown in Fig. 7A-C. Compared with those in the KO-NC group, the AOD values of Ki67, PCNA, and IL-33 in the colons of the mice in the KO-CAC group were significantly increased ($P<0.05$) (Fig. 7D-F). Compared with those in the KO-CAC group, the AOD values of Ki67, PCNA, and IL-33 in the colons of the mice in the KO-MOX group were significantly lower ($P<0.05$), suggesting that moxibustion could inhibit tumor cell proliferation and local inflammation in *kdm4d*^{-/-} mice.

Immunofluorescence staining of colonic β -Catenin is shown in Fig. 8A. Compared with that in the KO-NC group, the fluorescence intensity of β -Catenin in the

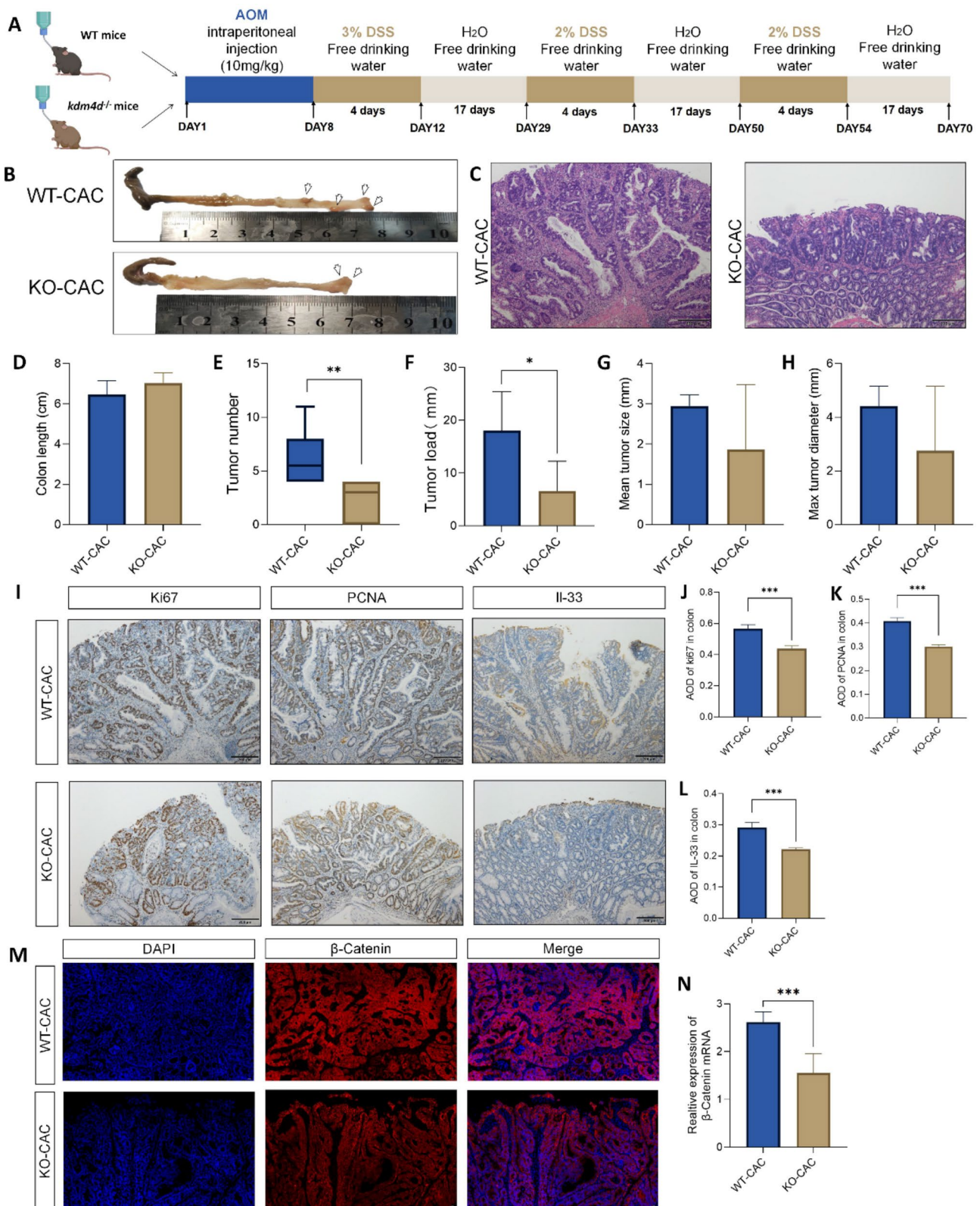


Fig. 5 (See legend on next page.)

(See figure on previous page.)

Fig. 5 Effects of *kdm4d* gene knockout on colon tumorigenesis in CAC mice. **A** Schematic protocol for the experiments. **B** Macroscopic observation of the colons of the mice in each group; the formation of colonic tumors is indicated by white arrows. **C** HE staining of the colons of the mice in each group (scale bars, 200 μ m). **D-H** Comparison of colon length, tumor number, tumor load, mean tumor diameter and maximum tumor diameter. **I** Ki67, PCNA and IL-33 expression in colon tumors (scale bars, 200 μ m). **J-L** AOD values of Ki67, PCNA and IL-33 in colon tumors. **M** β -Catenin expression in colon tumors (scale bars, 50 μ m). **N** represents the relative expression level of β -Catenin mRNA in colon tumors. $n=6$, compared with the WT-CAC group, * $P<0.05$, ** $P<0.01$, *** $P<0.001$

colons of the mice in the KO-CAC and KO-MOX group were greater. There was no difference in the fluorescence intensity of colon β -Catenin between KO-CAC and KO-MOX groups. RT-qPCR results showed that the relative expression of colonic β -Catenin mRNA was significantly increased in mice in the KO-CAC group compared with KO-NC ($P<0.05$). While there was no significant difference in the relative expression of colonic β -Catenin mRNA in mice in the KO-CAC and KO-MOX groups (Fig. 8B). These results suggest that in *kdm4d*^{-/-} mice, the effect of moxibustion on β -Catenin inhibition is reduced. KDM4D/ β -Catenin may constitute a signaling pathway through which moxibustion inhibits the proliferation of CAC tumors.

KDM4D/ β -Catenin participates in the process of moxibustion to regulate lipid metabolism in the CAC colon

To observe the effect of KDM4D on colonic lipid metabolism in CAC, sequencing data of colonic lipid metabolism in WT-NC, WT-CAC, and KO-CAC mice were analyzed. PCA and heatmap revealed differences in colonic lipid metabolism among the three groups (Fig. 9A and B). The volcano plot results revealed that, compared with those in the WT-CAC group, there were 74 significantly upregulated lipids and 46 significantly downregulated lipids in the KO-CAC group (Fig. 9C). The Venn diagram revealed that, compared with the WT-NC group, 72 lipids were downregulated in the WT-CAC group and upregulated in the KO-CAC group (Fig. 9D). Compared with the WT-NC group, 23 lipids were upregulated in the WT-CAC group and downregulated in the KO-CAC group (Fig. 9E). Among the 95 above mentioned lipids, 40 were significantly different in both the WT-NC and WT-CAC groups and the WT-CAC and KO-CAC groups (Supplementary Fig. S5). Compared with those in the WT-NC group, the contents of Cer(d20:1/24:0), Cer(d18:1/26:0), PC(18:1/22:3), SM(d18:1/14:1), SM(d18:1/26:0), and TAG52:0(18:0) lipids in the colons of the WT-CAC group were significantly greater ($P<0.05$) and were significantly lower in the KO-CAC group than in the WT-CAC group ($P<0.05$). Compared with those in the WT-NC group, the contents of 19 lipids, including TAG50:6(20:4), TAG58:7(18:0), TAG48:2(18:0), and TAG46:1(16:0), were significantly lower in the WT-CAC group ($P<0.05$), whereas the contents of these lipids in the KO-CAC group were significantly increased ($P<0.05$). These results suggest that these 40 lipids may be potential lipid

markers for the inhibition of CAC colon tumor proliferation by *kdm4d* knockout.

Next, we compared the effects of moxibustion on colonic lipid metabolism in *kdm4d*^{-/-} mice. The volcano plots and heatmap did not show a clear trend of discrete lipid metabolites in the three groups of mice (Fig. 9F and G). These findings suggest that the regulatory effect of moxibustion on lipid metabolism in the CAC colon is partially impaired in *kdm4d*^{-/-} mice.

To explore whether the effect of moxibustion on colonic lipid metabolism in CAC mice was related to the regulation of the KDM4D/ β -Catenin signaling pathway, we compared the potential lipid markers of moxibustion and KDM4D in the regulation of CAC (Fig. 4I and Supplementary Fig. S5). The results revealed that both moxibustion and *kdm4d* knockout had consistent effects on TAG58:7(18:0) and SM(d18:1/26:0). Compared with that in the WT-NC group, the SM(d18:1/26:0) in the WT-CAC group was significantly greater ($P<0.05$), and the SM(d18:1/26:0) in the WT-MOX and KO-CAC groups was significantly lower ($P<0.05$) (Fig. 9H). Compared with that in the WT-NC group, the content of TAG58:7 (18:0) in the WT-CAC group was significantly lower ($P<0.05$), whereas the content of TAG58:7 (18:0) in the WT-MOX and KO-CAC groups was significantly greater ($P<0.05$) (Fig. 9I). Spearman's correlation analysis was subsequently performed on the expression levels of KDM4D and β -Catenin mRNAs and the TAG58:7(18:0) and SM(d18:1/26:0) contents. The results revealed a significant positive correlation between the content of SM(d18:1/26:0) and the mRNA expression levels of KDM4D and β -Catenin ($P<0.05$) (Fig. 9J-K); there was a significant negative correlation between the content of TAG58:7(18:0) and the mRNA expression levels of KDM4D and β -Catenin ($P<0.05$) (Fig. 9L-M). These results suggest that TAG58:7(18:0) and SM(d18:1/26:0) may be involved in the pathway by which moxibustion regulates the KDM4D/ β -Catenin signaling pathway and inhibits the proliferation of CAC tumors (Fig. 9N).

Discussion

Inflammatory bowel disease (IBD), which includes ulcerative colitis and Crohn's disease, is characterized by chronic recurrent intestinal inflammation. IBD is a known risk factor for CAC. In recent years, owing to the optimization of early diagnosis and treatment technologies for IBD patients, the incidence of CAC has been

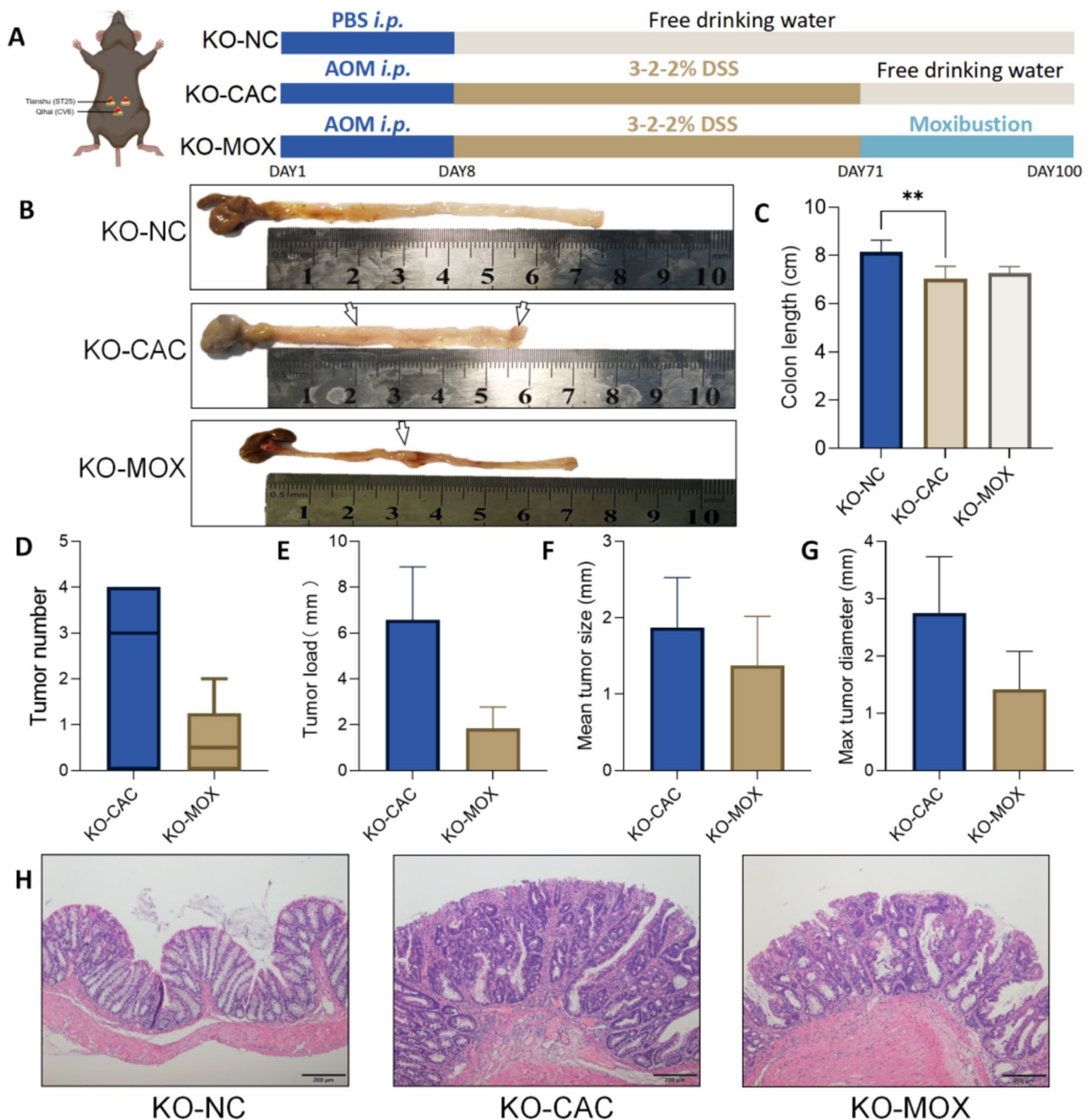


Fig. 6 Effects of moxibustion on colon tumorigenesis in *kdm4d*^{-/-} CAC mice. **A** Schematic protocol for the experiments. **B** Macroscopic observation of the colons of the mice in each group; the formation of colonic tumors is indicated by white arrows. **C** Comparison of colon length. **D-G** Comparison of tumor number, tumor load, mean tumor diameter and maximum tumor diameter. **H** HE staining of the colons of the mice in each group (scale bars, 200 μ m). $n=6$, compared with the KO-NC group, ** $P<0.01$

decreasing annually, and the incidence of colorectal cancer in IBD patients is still higher than that in the general population [6]. CAC is the main cause of death and the reason for colectomy in IBD patients [22], accounting for 10–15% of the deaths in this population [23]. Therefore, revealing the pathogenesis of CAC, slowing the progression of inflammation to cancer, and inhibiting the

proliferation of CAC tumors are very important for the clinical management of CAC. In this study, we explored the effect of moxibustion on colon tumor proliferation in mice with CAC induced by AOM combined with DSS. IL-33 is an epithelial cell-derived cytokine that plays an important role in intestinal immunity [24]. The upregulation of IL-33 expression was observed in colon tissues of

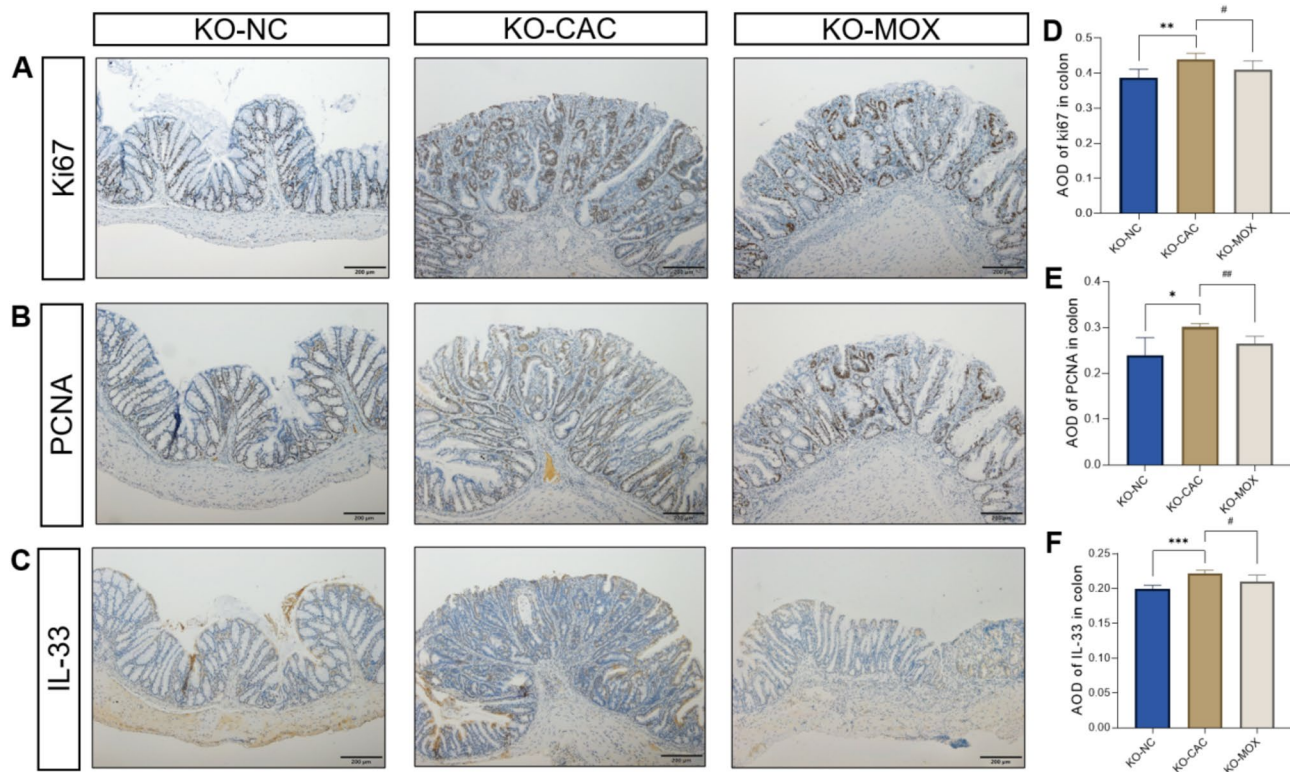


Fig. 7 Effects of moxibustion on the expression of proliferation-related proteins and IL-33 in the CAC tumors of *kdm4d*^{-/-} mice. **A-C** Ki67, PCNA and IL-33 expression in colon tumors (scale bars, 200 μ m). **D-F** AOD values of Ki67, PCNA and IL-33 in colon tumors. $n = 6$, compared with the KO-NC group, * $P < 0.05$, ** $P < 0.01$, *** $P < 0.001$; compared with the KO-CAC group, # $P < 0.05$, ## $P < 0.01$

both CRC and CAC mice and was positively correlated with tumor proliferation in CRC [25, 26]. We observed that moxibustion reduced the CAC tumor load and colon damage, inhibited the expression of the cell proliferation markers Ki67 and PCNA, and reduced the protein expression of the proinflammatory cytokine IL-33.

KDM4D has been proven to promote the occurrence and development of various digestive tract tumors [8, 9]. High expression of KDM4D in colorectal cancer metastases indicates poor prognosis [27]. KDM4D can activate the Wnt/ β -Catenin signaling pathway and promote the proliferation, migration, and invasion of CRC cells and the formation of colorectal tumors [11]. The results of this study revealed that moxibustion reduced the protein and mRNA expression of KDM4D and β -Catenin in CAC mice. These findings suggest that the inhibition of CAC tumor proliferation by moxibustion may be related to the inhibition of the KDM4D/ β -Catenin signaling pathway.

Metabolic reprogramming refers to changes in metabolic patterns in response to cellular energy requirements [28]. Metabolic reprogramming not only promotes the process of colon cancer transformation but also inevitably results in the process of colon cancer transformation. Lipid metabolism affects various biological processes, such as tumor cell growth, proliferation, migration, autophagy, and apoptosis [29]. In CRC, lipid

metabolism is involved in processes such as cell signal transduction, proinflammatory signal transduction, disruption of energy homeostasis, and dysregulation of membrane homeostasis [30]. Metabolomics can be used to systematically detect changes in metabolites and identify new potential biomarkers [31]. In this study, LC-MS lipid metabolomics technology was used to semiquantitatively detect lipid substances in the colons of mice, which is helpful for understanding lipid metabolism in CAC and screening potential targets for moxibustion to inhibit CAC tumor proliferation. Compared with those in the WT-NC group, 69 lipids were significantly upregulated and 154 were significantly downregulated in the colons of the WT-CAC group, and lipid metabolism homeostasis was widely disrupted. Compared with those in the WT-CAC group, 22 significantly upregulated lipids and 17 significantly downregulated lipids were detected in the colons of the WT-MOX group. Further comparison of the differential lipids in the three groups revealed that moxibustion modulated the levels of abnormally altered TAG56:7 (18:0), TAG58:7 (18:0), TAG55:1 (16:0), TAG56:1(16:0), TAG56:2 (18:0), SM (d18:1/26:0), SM(d18:1/22:1), DAG(16:0/22:3), PA(16:0/20:5) and PE(18:1/22:1) lipids in CAC.

There are several triacylglycerols (TAGs) among the above 10 lipids that may be associated with the inhibition

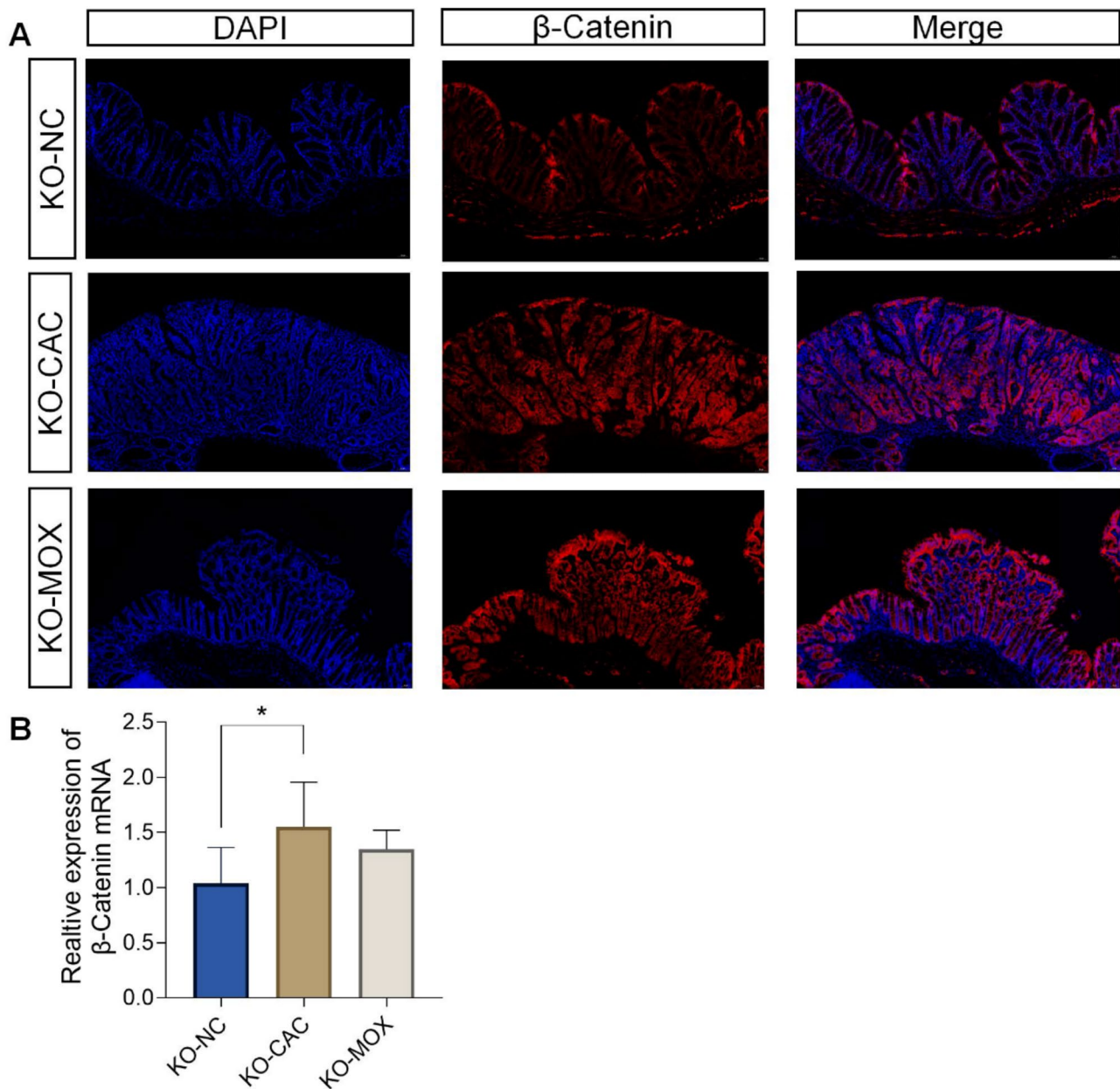


Fig. 8 Effects of moxibustion on the protein and mRNA expression of β -Catenin in the CAC tumors of *kdm4d*^{-/-} mice. **A** β -Catenin expression in colon tumors (scale bars, 50 μ m). **B** The relative expression level of β -Catenin mRNA in colon tumors. *n* = 6, compared with the KO-NC group, **P* < 0.05

of colon tumor proliferation in CAC mice by moxibustion. TAGs store high levels of metabolic energy. Dietary TAG is hydrolyzed and esterified in the intestine, combines with cholesterol and proteins in the form of chylomicrons, and is ultimately released into the bloodstream [32]. Currently, the role of TAG in CAC is unclear. Some studies have shown that changes in TAG content can be used to distinguish CAC tumor tissues from nonlesioned tissues. Compared with normal adjacent tissues, CAC tumor tissues present decreased TAG levels [33, 34]. This decrease may be related to the increased demand for energy production and cell membrane lipids owing to the

rapid proliferation of tumor cells. In this study, moxibustion also restored the levels of TAG56:7 (18:0), TAG58:7 (18:0), TAG55:1 (16:0), and TAG56:2 (18:0) in CAC mice. These findings suggest that moxibustion can reduce the demand for TAG as an energy substrate in mice with CAC.

KEGG results revealed that WT-NC and WT-CAC differential lipids and WT-CAC and WT-MOX differential lipids were enriched for choline metabolism in cancer and glycerophospholipid metabolism. There is a close relationship between choline metabolism and CRC, and the active proliferation of tumor cells requires

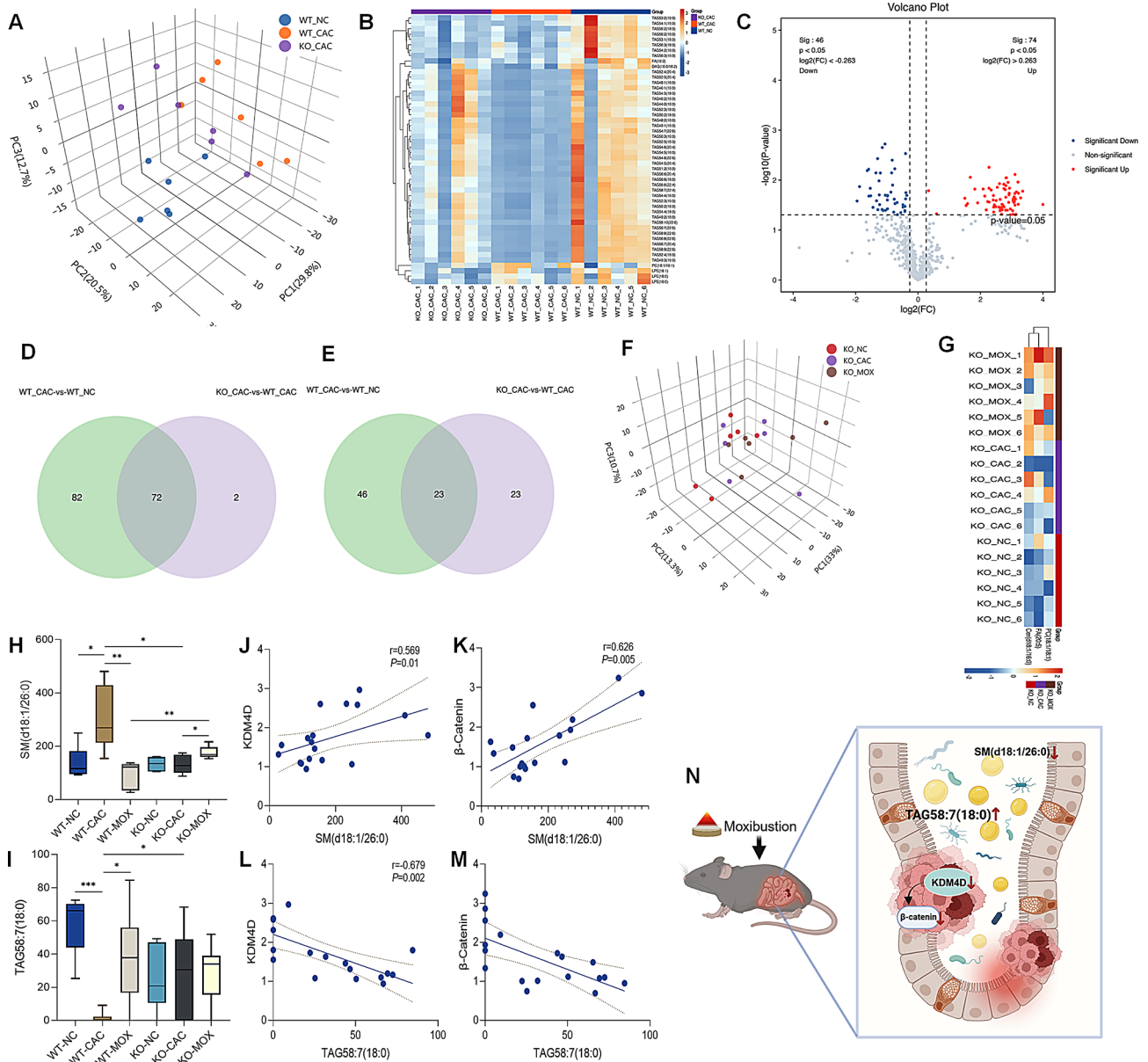


Fig. 9 Consistent effects of moxibustion and *kdm4*^{-/-} on colonic lipid metabolism in CAC. **A** 3D-PCA diagram of the WT-NC, WT-CAC and KO-CAC groups. **B** Heatmap of differential lipids in the colons of the WT-NC, WT-CAC, and KO-CAC. **C** Volcano plot of colonic differential lipids between the WT-CAC group and the KO-CAC group. The red dots represent lipids upregulated in the KO-CAC group compared with the WT-CAC group, and the blue dots represent lipids downregulated in the KO-CAC group compared with the WT-CAC group. **D** Venn diagram of lipids significantly downregulated in the WT-CAC group compared with the WT-NC group and significantly upregulated in the KO-CAC group compared with the WT-CAC group. **E** Venn diagram of lipids significantly upregulated in the WT-CAC group compared with the WT-NC group and significantly downregulated in the KO-CAC group compared with the WT-CAC group. **F** 3D-PCA diagram of the KO-NC, KO-CAC and KO-MOX groups. **G** Heatmap of differential lipids in the colons of the KO-NC, KO-CAC, and KO-MOX groups. **H** Comparison of SM (d18:1/26:0) content in the colons of the mice. **I** Comparison of TAG58:7(18:0) content in the colons of the mice. **J** Spearman's correlation analysis between SM(d18:1/26:0) and KDM4D mRNA. **K** Spearman's correlation analysis between SM(d18:1/26:0) and β -Catenin mRNA. **L** Spearman's correlation analysis between TAG58:7(18:0) and KDM4D mRNA. **M** Spearman's correlation analysis between TAG58:7(18:0) and β -Catenin mRNA. **N** Graphical example of how moxibustion affects colon KDM4D/ β -Catenin and lipid metabolism. $n=6$, $^*P<0.05$, $^{**}P<0.01$, $^{***}P<0.001$

the conversion of large amounts of choline into phosphatidylcholine for cell membrane synthesis [35]. The CRC gut microbiome contains an abundance of choline-degrading genes (*cutC* and *cutD*) [36]. Aberrant choline metabolism in tumors is accompanied by elevated

levels of the choline metabolites choline phosphate and glycerophosphocholine, which may serve as markers of metabolic reprogramming in cancer [35]. However, the glycerophospholipid metabolic pathway is a conserved metabolic pathway in humans and mice, and activation of

the glycerophospholipid metabolic pathway accelerates the progression of CRC and CAC [37], which may also serve as a biomarker for monitoring CRC patients [38]. The abovementioned studies suggest that choline metabolism and glycerophospholipid metabolism play a role in the reprogramming of lipid metabolism in colon carcinogenesis and that the modulatory effects of moxibustion in CAC mice may be related to choline metabolism and glycerophospholipid metabolism.

Next, we explored the relationship between the KDM4D/ β -Catenin pathway and the inhibition of CAC tumor proliferation by moxibustion in *kdm4d*^{-/-} mice. The results showed that after *kdm4d* knockout, the tumor number and load in CAC mice were significantly reduced, which is consistent with the findings of previous studies [10]. Additionally, the expression levels of PCNA, Ki67, and IL-33 and the fluorescence intensity of β -Catenin in the colons of KO-CAC mice were reduced. However, in *kdm4d* knockout mice, the effect of moxibustion in inhibiting tumor proliferation was affected to a certain extent. Moxibustion failed to significantly reduce the number and burden of tumors in CAC mice and had no significant effect on β -Catenin expression. These results show that activation of the KDM4D/ β -Catenin signaling pathway plays an important role in promoting CAC tumor proliferation. The inhibition of KDM4D/ β -Catenin signaling may be one of the mechanisms by which moxibustion inhibits CAC tumor proliferation.

The lipid metabolism pathway in tumor cells is regulated by multiple signaling pathways, such as the Wnt, Notch, Hippo, and Hedgehog pathways. In CRC, a high-fat diet and dysregulated Wnt/ β -Catenin signaling pathway could change the intestinal bile acid profile, activate the farnesoid X receptor (FXR), and drive the malignant transformation of Lgr5-expressing cancer stem cells, thereby promoting progression from adenoma to adenocarcinoma [39]. Therefore, it is important to explore the interaction between the KDM4D/ β -Catenin signaling pathway and lipid metabolism to understand the pathogenesis of CAC.

An analysis of the changes in colonic lipids in the WT-NC, WT-CAC, and KO-CAC groups revealed the influence of KDM4D on colonic lipid metabolism in CAC mice. Compared with those in the other two groups, 40 lipids were significantly upregulated or downregulated in the WT-CAC. Specifically, compared with those in the WT-CAC group, there was a significant increase in various glycerides (specifically triacylglycerols) and a significant decrease in various sphingolipids (specifically ceramides) in the colons of the mice in the KO-CAC group. In the colons of *kdm4d*^{-/-} mice, the levels of various long-chain polyunsaturated triacylglycerols were also significantly increased. These findings suggest that knockout of the *kdm4d* gene may have a similar effect

to that of moxibustion in terms of reducing the energy demand required for colon tumor proliferation in CAC. However, in the three groups of *kdm4d*^{-/-} mice, we did not observe an obvious discrete trend in the lipid levels. The regulatory effect of moxibustion on lipid metabolites in CAC mice was weakened by *kdm4d* knockout. *kdm4d* may be a key moxibustion gene affecting lipid metabolism in CAC.

To explore the relationship between moxibustion inhibition of the KDM4D/ β -Catenin signaling pathway and lipid metabolism, we compared 10 lipid markers of moxibustion and 40 lipid markers in *kdm4d* knockout mice. The results showed that moxibustion and *kdm4d*^{-/-} had consistent effects on TAG58:7(18:0) and SM(d18:1/26:0) levels. The results revealed a significant correlation between the contents of SM (d18:1/26:0) and TAG58:7 (18:0) and the mRNA expression levels of KDM4D and β -Catenin. Sphingomyelin (SM) is a major component of various biological membranes and is involved in regulating cell membrane stability and secretory activity. SM can promote the development and progression of multiple cancers by regulating cell proliferation and migration [40]. Conversely, the inhibition of SM synthesis inhibits CRC metastasis [41]. These findings indicate that SM(d18:1/26:0), a lipid metabolite, may be closely related to the regulation of the KDM4D/ β -Catenin signaling pathway and the inhibition of CAC tumor proliferation.

Conclusions

This is the first study to report the mechanism by which moxibustion inhibits the proliferation of CAC tumors from the perspectives of KDM4D and lipid metabolism. In this study, we observed that moxibustion inhibited the proliferation of CAC tumors and the expression of colon KDM4D and β -Catenin. Abnormal lipid metabolism was observed in the colon of CAC mice. *Kdm4d* may be one of the key genes that regulates lipid metabolism in the CAC colon. Moxibustion can inhibit abnormal activation of the KDM4D/ β -Catenin signaling pathway and regulate lipid substances such as sphingomyelin SM(d18:1/26:0) to inhibit tumor proliferation in CAC mice.

Supplementary Information

The online version contains supplementary material available at <https://doi.org/10.1186/s12935-025-03798-8>.

Supplementary Material 1: Additional file 1: Table S1 Primer sequences for β -actin, KDM4D and β -Catenin. Figure S1 Identification of *kdm4d* gene knockout. Mice showing a band only in panel A and no band in panel B are classified as *kdm4d*^{-/-}. Those exhibiting a band only in panel B and no band in panel A are designated as wt/wt. Mice presenting bands in both panels A and B are identified as heterozygous. Figure S2 AOM combined with DSS resulted in CAC tumorigenesis. A Macroscopic observation of the colons of NC and CAC mice; the formation of colonic tumors is indicated by white arrows. B HE staining of the colons of NC and CAC mice (left scale bars, 500 μ m; right scale bars, 100 μ m). Figure S3 AOM combined with DSS induced CAC tumorigenesis in *kdm4d* knockout mice. A Macroscopic

observation of the colons of NC and CAC mice; the formation of colonic tumors is indicated by white arrows. B Histopathological examination of mouse colon tissues (left scale bars, 500 μm ; right scale bars, 100 μm). Figure S4 Quality assessment of the lipid pseudotargeted lipid metabolomics data. A 2D-PCA diagram. B 3D-PCA diagram. C QC-corrplot plot. D NEG chromatograms of OC samples. E POS chromatograms of the QC samples. Figure S5 Box plots of differential lipids in the WT-NCWT-CAC and KO-CAC groups. * $P < 0.05$, ** $P < 0.01$, *** $P < 0.001$.

Acknowledgements

The authors thank Oebiotech for their help with the detection of the LC-MS lipid metabolism profiles. The authors thank Springer Nature Author Services for English language editing (No. B66F-A795-661B-1376-FEE5). The images of the mice shown in Fig. 1 and Fig. 6, and graphs of Fig. 3D, Fig. 5 A and Fig. 9 N were obtained from Biorender.com (Agreement number: KU282L5UHA).

Author contributions

GL, YH and HW designed the study. GL, JM, LW, HZ, YL, LK, MG and HD contributed to the experiments. GL, JM, HD, HX and YH performed the data collection and data analysis. HW, YL and KL provided funding. GL and LW drafted the manuscript. YH and HD provided writing, review and editing. All the authors read and approved the final manuscript.

Funding

This study was supported by the National Natural Science Foundation of China (No. 81973953, 82205293, and 82205261), High level Traditional Chinese Medicine Key Subjects of the State Administration of Traditional Chinese Medicine (No. zyyzdxk-2023068) and Shanghai Clinical Research Center for Acupuncture and Moxibustion (No. 20MC1920500).

Data availability

No datasets were generated or analysed during the current study.

Declarations

Ethics approval and consent to participate

All operations were approved by the SHUTCM (NO. PZSHUTCM2305180004 and PZSHUTCM220725005) and complied with relevant regulations on animal ethics.

Consent for publication

All the authors have agreed to publish this manuscript.

Competing interests

The authors declare no competing interests.

Author details

¹Yueyang Hospital of Integrative Chinese and Western Medicine, Shanghai University of Traditional Chinese Medicine, 110 Ganhe Road, Shanghai 200437, China

²Shanghai Research Institute of Acupuncture and Meridian, Shanghai University of Traditional Chinese Medicine, 650 Wanping Road, Shanghai 200030, China

³Shanghai Guanghua Hospital of Integrated Traditional Chinese and Western Medicine, Shanghai University of Traditional Chinese Medicine, 568 Xinhua Road, Shanghai 200052, China

Received: 10 January 2025 / Accepted: 22 April 2025

Published online: 05 May 2025

References

- Cassidy S, Syed BA. Colorectal cancer drugs market. *Nat Rev Drug Discov*. 2017;16:525–6.
- Siegel RL, Miller KD, Wagle NS, Jemal A. Cancer statistics, 2023. *CA Cancer J Clin*. 2023;73:17–48.
- Siegel RL, Wagle NS, Cercek A, Smith RA, Jemal A. Colorectal cancer statistics, 2023. *CA Cancer J Clin*. 2023;73:233–54.
- Lasry A, Zinger A, Ben-Neriah Y. Inflammatory networks underlying colorectal cancer. *Nat Immunol*. 2016;17:230–40.
- Tan G, Huang C, Chen J, Zhi F. HMGB1 released from GSDME-mediated pyroptotic epithelial cells participates in the tumorigenesis of colitis-associated colorectal cancer through the ERK1/2 pathway. *J Hematol Oncol*. 2020;13:149.
- Shah SC, Itzkowitz SH. Colorectal Cancer in inflammatory bowel disease: mechanisms and management. *Gastroenterology*. 2022;162:715–e7303.
- Tan Y, Lin J, Li T, Li J, Xu R, Ju H. LncRNA-mediated posttranslational modifications and reprogramming of energy metabolism in cancer. *Cancer Commun (Lond)*. 2020;41:109–20.
- Hu F, Li H, Liu L, Xu F, Lai S, Luo X, et al. Histone demethylase KDM4D promotes Gastrointestinal stromal tumor progression through HIF1 β /VEGFA signalling. *Mol Cancer*. 2018;17:107.
- Chen Q, Zhuang S, Hong Y, Yang L, Guo P, Mo P, et al. Demethylase JMJD2D induces PD-L1 expression to promote colorectal cancer immune escape by enhancing IFNGR1-STAT3-IRF1 signaling. *Oncogene*. 2022;41:1421–33.
- Peng K, Kou L, Yu L, Bai C, Li M, Mo P, et al. Histone demethylase JMJD2D interacts with β -Catenin to induce transcription and activate colorectal Cancer cell proliferation and tumor growth in mice. *Gastroenterology*. 2019;156:1112–26.
- Zhuo M, Chen W, Shang S, Guo P, Peng K, Li M, et al. Inflammation-induced JMJD2D promotes colitis recovery and colon tumorigenesis by activating Hedgehog signaling. *Oncogene*. 2020;39:3336–53.
- Wang T, Fahrman JF, Lee H, Li Y-J, Tripathi SC, Yue C, et al. JAK/STAT3-Regulated fatty acid β -Oxidation is critical for breast Cancer stem cell Self-Renewal and chemoresistance. *Cell Metab*. 2018;27:136–e1505.
- Bacci M, Lorito N, Smiraglia A, Morandi A. Fat and Furious: lipid metabolism in antitumoral therapy response and resistance. *Trends Cancer*. 2021;7:198–213.
- Lu S, Wang B, Wang J, Guo Y, Li S, Zhao S, et al. Moxibustion for the treatment of Cancer and its complications: efficacies and mechanisms. *Integr Cancer Ther*. 2023;22:15347354231198089.
- Li Y, Hong E, Ye W, You J. Moxibustion as an adjuvant therapy for Cancer pain: A systematic review and Meta-Analysis. *J Pain Res*. 2023;16:515.
- Li G, Zhao C, Xu J, Huang Y, Qiao Y, Li F, et al. Moxibustion alleviates intestinal inflammation in ulcerative colitis rats by modulating long non-coding RNA LOC108352929 and inhibiting Phf11 expression. *Heliyon*. 2024;10:e26898.
- Xu H, Wang Y, Xu J, Huang Y, Qiao Y, Li F, et al. Study on the mechanism of herb cake-partitioned moxibustion inhibiting tumor growth in colitis-associated colorectal cancer based on KDM4D receptor. *J Acupunct Tuina Sci*. 2024;22:1–11.
- Greten FR, Eckmann L, Greten TF, Park JM, Li Z-W, Egan LJ, et al. IKK β links inflammation and tumorigenesis in a mouse model of colitis-associated cancer. *Cell*. 2004;118:285–96.
- Deng Y, Li M, Zhuo M, Guo P, Chen Q, Mo P, et al. Histone demethylase JMJD2D promotes the self-renewal of liver cancer stem-like cells by enhancing EpCAM and Sox9 expression. *J Biol Chem*. 2021;296:100121.
- Bai B, Wu F, Ying K, Xu Y, Shan L, Lv Y, et al. Therapeutic effects of Dihydroartemisinin in multiple stages of colitis-associated colorectal cancer. *Theranostics*. 2021;11:6225–39.
- Dzhallilova D, Zolotova N, Fokichev N, Makarova O. Murine models of colorectal cancer: the azoxymethane (AOM)/dextran sulfate sodium (DSS) model of colitis-associated cancer. *PeerJ*. 2023;11:e16159.
- Zhou RW, Harpaz N, Itzkowitz SH, Parsons RE. Molecular mechanisms in colitis-associated colorectal cancer. *Oncogenesis*. 2023;12:1–11.
- Mattar MC, Lough D, Pishvaian MJ, Charabaty A. Current management of inflammatory bowel disease and colorectal Cancer. *Gastrointest Cancer Res*. 2011;4:53–61.
- Jou E, Rodriguez-Rodriguez N, McKenzie ANJ. Emerging roles for IL-25 and IL-33 in colorectal cancer tumorigenesis. *Front Immunol*. 2022;13:981479.
- Li Y, Shi J, Qi S, Zhang J, Peng D, Chen Z, et al. IL-33 facilitates proliferation of colorectal cancer dependent on COX2/PGE2. *J Exp Clin Cancer Res*. 2018;37:196.
- Islam MS, Horiguchi K, Iino S, Kaji N, Mikawa S, Hori M, et al. Epidermal growth factor is a critical regulator of the cytokine IL-33 in intestinal epithelial cells. *Br J Pharmacol*. 2016;173:2532.
- Wu X, Li R, Song Q, Zhang C, Jia R, Han Z, et al. JMJD2C promotes colorectal cancer metastasis via regulating histone methylation of MALAT1 promoter and enhancing β -catenin signaling pathway. *J Exp Clin Cancer Res*. 2019;38:435.
- Heiden MG, DeBerardinis RJ. Understanding the intersections between metabolism and cancer biology. *Cell*. 2017;168:657–69.

29. Gong J, Lin Y, Zhang H, Liu C, Cheng Z, Yang X, et al. Reprogramming of lipid metabolism in cancer-associated fibroblasts potentiates migration of colorectal cancer cells. *Cell Death Dis.* 2020;11:267.
30. Salita T, Rustam YH, Mouradov D, Sieber OM, Reid GE. Reprogrammed lipid metabolism and the lipid-Associated hallmarks of colorectal Cancer. *Cancers (Basel).* 2022;14:3714.
31. Hang D, Zeleznik OA, Lu J, Joshi AD, Wu K, Hu Z, et al. Plasma metabolomic profiles for colorectal cancer precursors in women. *Eur J Epidemiol.* 2022;37:413–22.
32. Pakiet A, Kobiela J, Stepnowski P, Sledzinski T, Mika A. Changes in lipids composition and metabolism in colorectal cancer: a review. *Lipids Health Dis.* 2019;18:29.
33. Pakiet A, Sikora K, Kobiela J, Rostkowska O, Mika A, Sledzinski T. Alterations in complex lipids in tumor tissue of patients with colorectal cancer. *Lipids Health Dis.* 2021;20:85.
34. Mika A, Pakiet A, Czumaj A, Kaczynski Z, Liakh I, Kobiela J, et al. Decreased triacylglycerol content and elevated contents of cell membrane lipids in colorectal Cancer tissue: A lipidomic study. *J Clin Med.* 2020;9:1095.
35. Han Z, Gu J, Xin J, Liu H, Wu Y, Du M, et al. Genetic variants in choline metabolism pathway are associated with the risk of bladder cancer in the Chinese population. *Arch Toxicol.* 2022;96:1729–37.
36. Avuthu N, Guda C. Meta-Analysis of altered gut microbiota reveals microbial and metabolic biomarkers for colorectal Cancer. *Microbiol Spectr.* 10:e00013–22.
37. Wang L, Tu Y, Chen L, Zhang Y, Pan X, Yang S, et al. Male-Biased gut Microbiome and metabolites aggravate colorectal Cancer development. *Adv Sci (Weinh).* 2023;10:2206238.
38. Lv J, Jia Y, Li J, Kuai W, Li Y, Guo F, et al. Gegen Qinlian Decoction enhances the effect of PD-1 Blockade in colorectal cancer with microsatellite stability by remodelling the gut microbiota and the tumour microenvironment. *Cell Death Dis.* 2019;10:415.
39. Fu T, Coulter S, Yoshihara E, Oh TG, Fang S, Cayabyab F, et al. FXR regulates intestinal cancer stem cell proliferation. *Cell.* 2019;176:1098–e111218.
40. Taniguchi M, Okazaki T. The role of sphingomyelin and sphingomyelin synthases in cell death, proliferation and migration-from cell and animal models to human disorders. *Biochim Biophys Acta.* 2014;1841:692–703.
41. Long X, Liu X, Deng T, Chen J, Lan J, Zhang S, et al. LARP6 suppresses colorectal cancer progression through ZNF267/SGMS2-mediated imbalance of sphingomyelin synthesis. *J Exp Clin Cancer Res.* 2023;42:33.

Publisher's note

Springer Nature remains neutral with regard to jurisdictional claims in published maps and institutional affiliations.